


In Vivo Validation Model of a Novel Anti-Inflammatory Scaffold in Interleukin-10 Knockout Mouse

Jung Yeon Kim¹ · So Young Chun¹ · Sang Hoon Lee² · Eugene Lih³ · Jeongshik Kim⁴ · Dae Hwan Kim⁵ · Yun-Sok Ha⁶ · Jae-Wook Chung^{6,7} · Jun Nyung Lee^{6,7} · Bum Soo Kim⁶  · Hyun Tae Kim^{6,7} · Eun Sang Yoo⁶ · Dong Keun Han³ · Tae Gyun Kwon^{6,7} · Byung Ik Jang²

Received: 4 January 2018 / Revised: 19 April 2018 / Accepted: 20 April 2018 / Published online: 23 June 2018

© The Korean Tissue Engineering and Regenerative Medicine Society and Springer Science+Business Media B.V., part of Springer Nature 2018

Abstract

BACKGROUND: We fabricated anti-inflammatory scaffold using Mg(OH)₂-incorporated polylactic acid-polyglycolic acid copolymer (MH-PLGA). To demonstrate the anti-inflammatory effects of the MH-PLGA scaffold, an animal model should be sensitive to inflammatory responses. The interleukin-10 knockout (IL-10 KO) mouse is a widely used bowel disease model for evaluating inflammatory responses, however, few studies have evaluated this mouse for the anti-inflammatory scaffold.

METHODS: To compare the sensitivity of the inflammatory reaction, the PLGA scaffold was implanted into IL-10 KO and C57BL/6 mouse kidneys. Morphology, histology, immunohistochemistry, and gene expression analyses were carried out at weeks 1, 4, 8, and 12. The anti-inflammatory effect and renal regeneration potency of the MH-PLGA scaffold was also compared to those of PLGA in IL-10 KO mice.

RESULTS: The PLGA scaffold-implanted IL-10 KO mice showed kidneys relatively shrunken by fibrosis, significantly increased inflammatory cell infiltration, high levels of acidic debris residue, more frequent CD8-, C-reactive protein-, and ectodysplasin A-positive cells, and higher expression of pro-inflammatory and fibrotic factors compared to the control group. The MH-PLGA scaffold group showed lower expression of pro-inflammatory and fibrotic factors, low immune cell infiltration, and significantly higher expression of anti-inflammatory factors and renal differentiation related genes compared to the PLGA scaffold group.

CONCLUSION: These results indicate that the MH-PLGA scaffold had anti-inflammatory effects and high renal regeneration potency. Therefore, IL-10 KO mice are a suitable animal model for *in vivo* validation of novel anti-inflammatory scaffolds.

Keywords IL-10 KO mice · Anti-inflammatory scaffold · Mg(OH)₂ · Renal regeneration · Fibrosis

Jung Yeon Kim and So Young Chun have contributed equally to this work.

Tae Gyun Kwon and Byung Ik Jang have contributed equally to this work as co-corresponding authors.

✉ Tae Gyun Kwon
tgkwon@knu.ac.kr

✉ Byung Ik Jang
jbi@med.yu.ac.kr

¹ Biomedical Research Institute, Kyungpook National University Hospital, 130 Dongdeok-ro, Jung-gu, Daegu 41944, South Korea

1 Introduction

When tissue or organ injury is out of the natural healing range, specific treatment is required to recover the original function and morphology. The most effective treatment from the perspective of regenerative medicine is combined therapy that uses both cells and a scaffold [1]. However, the available number of autologous cells is very limited, allogeneic cells cause immune rejection and complicated processing problems, and xenogeneic cell application is technically impossible [2, 3]. However, the use of a scaffold alone is advantageous for producing the required number of cells with adequate biocompatibility [4]. Thus, in clinical applications, implantation of a scaffold alone has become an important method.

The most widely used material for tissue regeneration is the polylactic acid-polyglycolic acid copolymer (PLGA)-based scaffold, which is synthetic, biodegradable, and biocompatible [5]. However, PLGA produces acidic debris when it degrades *in vivo*, and acidic conditions are the main causes of inflammatory responses [6]. This acute immune response inhibits host stem cell recruitment, survival, proliferation, and differentiation [7], and this early undesirable microenvironment can inhibit tissue regeneration. To overcome this problem, researchers incorporated magnesium hydroxide [$\text{Mg}(\text{OH})_2$] into the PLGA scaffold [8]. $\text{Mg}(\text{OH})_2$ is safe for handling and non-toxic [9], and thus may be useful for neutralizing the acidic environment. We manufactured an $\text{Mg}(\text{OH})_2$ -incorporated PLGA (MH-PLGA) scaffold for application in kidney regeneration.

In vivo experiments to test the anti-inflammatory effects of the MH-PLGA scaffold require an animal model that is sensitive to inflammatory responses. We used IL-10 knockout (IL-10 KO) mice because IL-10 is a representative anti-inflammatory and immunoregulatory cytokine that

downregulates activation of monocytes and macrophages [10]. IL-10 KO mice are widely used as a chronic inflammatory bowel disease model [11–13]; however, few studies have evaluated these mice with anti-inflammatory scaffolds. Here, we investigated whether IL-10 KO mice are a suitable animal model for evaluating the effectiveness of the anti-inflammatory MH-PLGA scaffold in kidney tissue regeneration.

2 Materials and methods

2.1 MH-PLGA scaffold preparation

The scaffold was kindly provided by Dr. Dong Keun Han (Korea Institute of Science and Technology, Seoul, Korea). Briefly, the scaffold was manufactured as follows using a freeze-drying method [8]. Ice microparticulates (100–150 μm) were prepared by spraying cold deionized water into liquid nitrogen. A 13% (w/v) solution of PLGA (MW = 40 kDa; Boehringer Ingelheim, Ingelheim, Germany) in methylene chloride was mixed with 0.15 g of $\text{Mg}(\text{OH})_2$ (Sigma-Aldrich, St Louis, MO, USA) nanoparticles [which were synthesized by the reaction of $\text{Mg}(\text{NO}_3)_2$ with NaOH. Five grams of $\text{Mg}(\text{NO}_3)_2$ and 1.6 g of NaOH were dissolved in 100 and 200 mL of dH_2O , and then, the $\text{Mg}(\text{NO}_3)_2$ solution was added to the NaOH solution. The precipitate was washed with dH_2O , collected by centrifugation and dried in a vacuum]. The solution was vortexed, and the ice microparticulates were added to pre-cooled PLGA solution. The mixture placed on a silicon mold in liquid nitrogen for freezing, and then freeze-dried for 2 days. The MH-PLGA scaffold was sterilized with ethylene oxide. The characterizations of scaffold for physical, chemical and biocompatibility were described in our previous report [8].

2.2 *In vivo* study design

All procedures were performed in accordance with an animal protocol approved by the Yeungnam University Institutional Animal Care and Use Committee (YUMC-AEC2014-030). IL-10 KO mice were purchased from The Jackson Laboratory (Bar Harbor, ME, USA) and bred under specific pathogen-free conditions in the laboratory animal center at the Yeungnam University Medical Center. For *in vivo* experiments, scaffolds were prewetted in absolute ethanol for 1 h and immersed in phosphate-buffered saline for 1 h. Mice (20 g, female) were randomly divided into 3 groups (each group $n = 20$): (1) Ctrl group: sham-operated C57BL/6 mice, (2) WT group: PLGA scaffold-implanted C57BL/6 mice (wild-type), and (3) IL-10 KO group: PLGA scaffold-implanted IL-10 KO mice.

² Department of Internal Medicine, Yeungnam University College of Medicine, 170 Hyunchung-ro, Nam-gu, Daegu 42415, South Korea

³ Department of Biomedical Science, CHA University, 335 Panyoro, Seongnam-si, Gyeonggi 13488, South Korea

⁴ Department of Pathology, Central Hospital, 480 Munsu-ro, Nam-gu, Ulsan 44667, South Korea

⁵ Department of Laboratory Animal Research Support Team, Yeungnam University Hospital, 170 Hyunchung-ro, Nam-gu, Daegu 42415, South Korea

⁶ Department of Urology, School of Medicine, Kyungpook National University, Kyungpook National University Hospital, 130 Dongdeok-ro, Jung-gu, Daegu 41944, South Korea

⁷ Department of Urology, Kyungpook National University Chilgok Hospital, 807 Hogukro, Bukgu, Daegu 41404, South Korea

Fig. 1 Surgical method and scaffold implantation. **A** Right kidney exposure. **B** Partial nephrectomy (excision volume, $5 \times 2 \times 2 \text{ mm}^3$). **C** Scaffold (size $5 \times 2 \times 2 \text{ mm}^3$) implantation

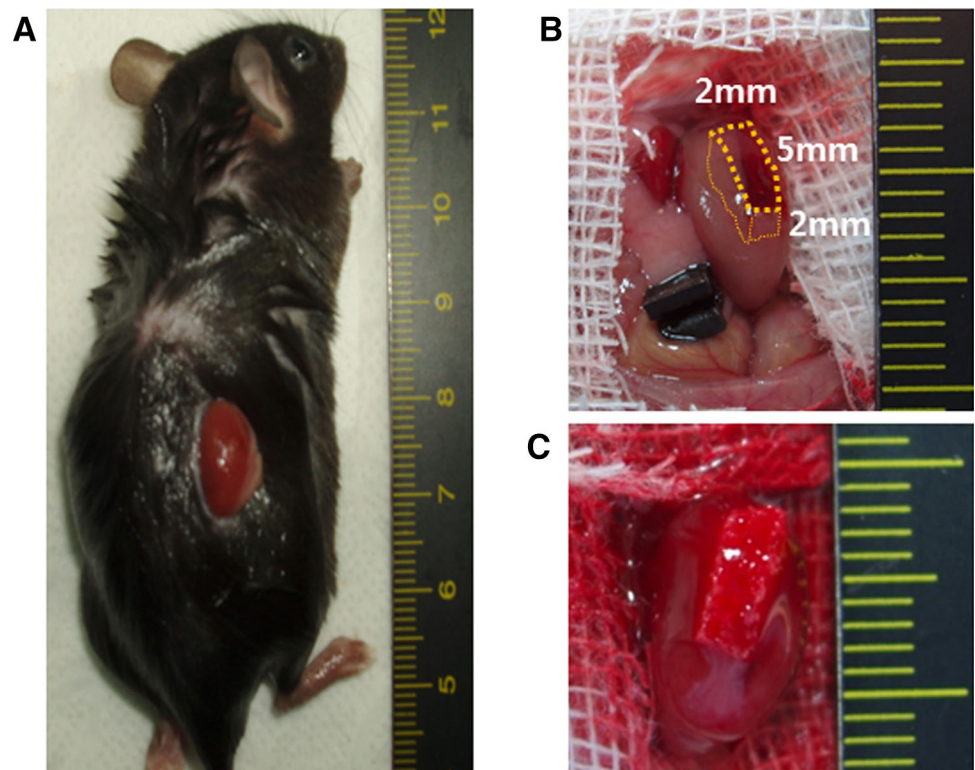


Table 1 Real-time PCR primer sequences

Function	Genes	Primers	
Renal regeneration	Wnt	ggagcctagcccggactc	gcagccgtcaatggcttag
	Pax2	aaatctctatgcaaaatgacgaacat	gagagatgcaggcgcgatgaa
	Wt1	ggtccgccatcacacatg	ctttctgctgggatgct
	Emx2	tggccagaaagccaaagc	tccgctcccaccacgtaat
	vWf	gctgtgcggtgatttaacatc	ccgtttacaccgctgttct
	Laminin	ggatggatgtcgaccatgtga	tgacgtccaatcatgtgaggc
	Col4	ccacttcccctcccttag	cccgggttttctgtgtct
	Krt10	tggcctctacatggacaaag	tggcttgagtgccatgct
	Cadherin	cagagggtggctctgtatc	ggactgggctgtgtacct
	Anti-inflammation	IL-4	tcaacccccagctagtgtc
IL-2		cccactcaagctccactc	atcctggggagttcagggt
TGF- β 1		ttgcttcagctccacagaga	tggttgtagaggcaaggac
Pro-inflammation	TNF- α	agccccagctctgtatcct	ctccccttcagaaactcagg
	IL-6	agttgcctcttgggactga	tccacgattcccagagaac
	MCP-1	aggtccctgcatgctcttg	tctggaccattcctcttg
Fibrosis	Vimentin	tccagatcgatgtggacgtt	atactgctggcgacatcac
	Col1	gagcggagagtactggatcg	gctcttttcttgggggtc
	FSP-1	gatgagcaactggacagca	atgtcggaagaagccagagt
	α -SMA	ctgacagaggcaccactgaa	catctccagagtcacagaca
Housekeeping	GAPDH	tgtgtccgtcgtggatctga	cctgcttcaccaccttcttga

Next, $\text{Mg}(\text{OH})_2$ -incorporated PLGA scaffold-implanted IL-10 KO mice (MH-PLGA group) were compared to PLGA scaffold-implanted IL-10 KO mice (PLGA group).

Mice were anesthetized with 3–4% isoflurane, and then the right kidney was exposed through an incision on the back (Fig. 1A) and subjected to partial nephrectomy (excision

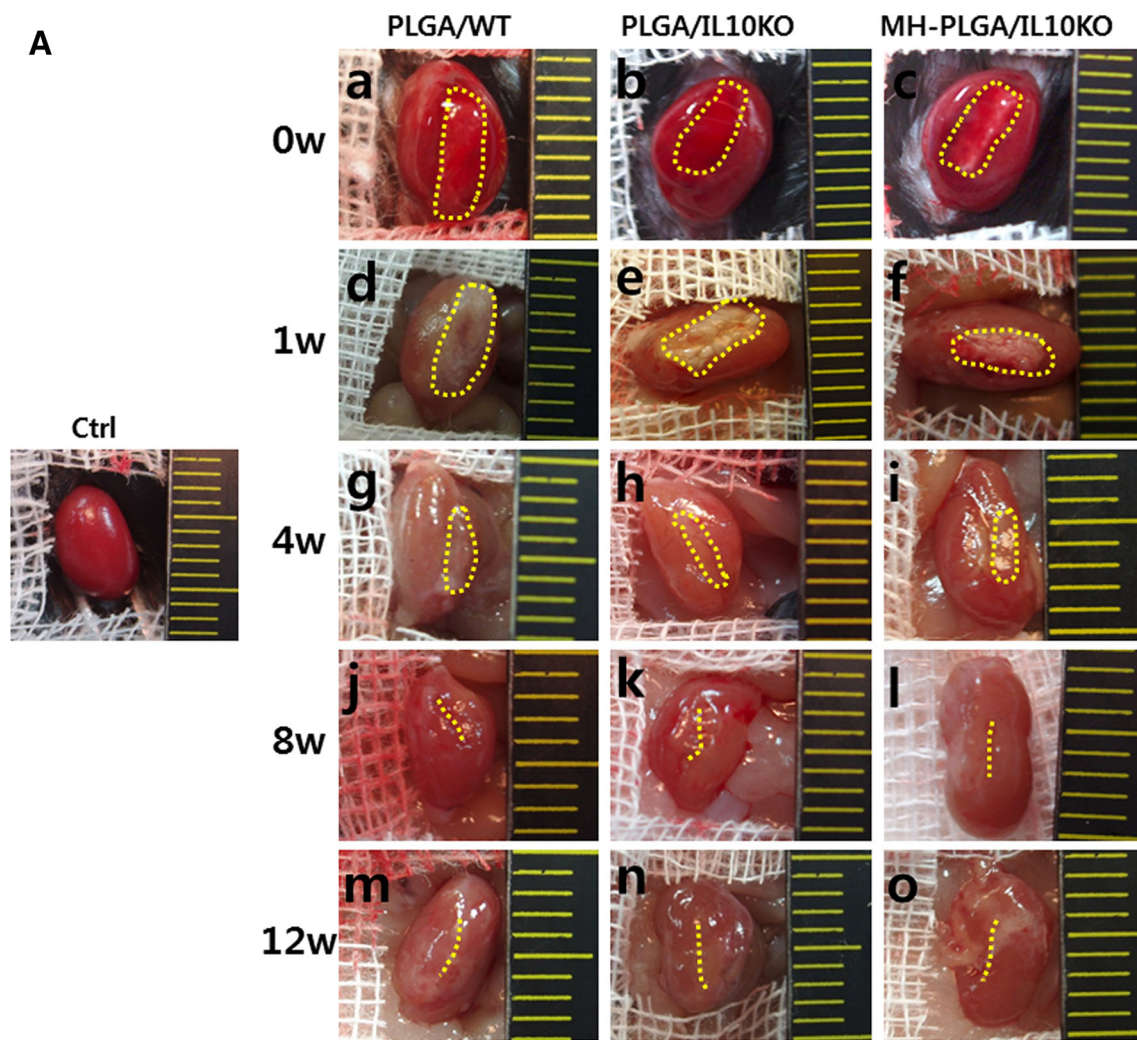


Fig. 2 Histological and immunohistochemical (IHC) analyses of inflammatory reactions. **A** Gross images of scaffold-implanted kidney. **B, C** H&E staining at 1, 4, 8, and 12 weeks after scaffold implantation **B** arrows in **a–c** are PLGA acidic debris, in **d–f** are empty space by PLGA degradation, **g–i** are inflammatory cells, and **j–l** are kidney progenitor cells. **C** Arrows in **a–c** are PLGA acidic debris, in **d–i** are formed glomeruli. **D–F** IHC analysis with CD8 antibody for detection of cytotoxic T cell, CRP antibody for monocytes, and CD68 antibody for macrophages (positive cells for

each antibody were indicated by arrow). Positively stained cell numbers per unit ($4860 \mu\text{m}^2$) are counted and graphed. Ctrl, sham-operated C57BL/6 mice; PLGA/WT, PLGA scaffold-implanted C57BL/6 mice; PLGA/IL10KO, PLGA scaffold-implanted IL-10KO mice; MH-PLGA/IL10KO, Mg(OH)₂-incorporated PLGA scaffold-implanted IL-10KO mice. H&E stain magnification; $\times 400$. * $p < 0.05$ (PLGA/IL10KO vs. PLGA/WT), # $p < 0.05$ (MH-PLGA/IL10KO vs. PLGA/IL10KO)

volume, $5 \times 2 \times 2 \text{ mm}^3$) (Fig. 1B) or sham operation. The scaffolds (size $5 \times 2 \times 2 \text{ mm}^3$) were implanted into the injured site (Fig. 1C). Kidneys were harvested at weeks 1, 4, 8, and 12 post-surgery.

2.3 Histology, immunohistochemistry, and gene expression analyses

For histological and immunohistochemical (IHC) analyses of inflammation-related factors, half of the kidney was fixed with 4% paraformaldehyde (5 mice/group). Paraffin-embedded samples were cut into 5- μm sections for

hematoxylin and eosin (H&E) and IHC staining. Histological analyses were performed for regenerated glomerular morphology (size, number, and location), renal tubule regeneration, inflammation-related cell infiltration, renal progenitor cell migration, scaffold debris distribution, angiogenesis, calcification, and scar formation. For IHC analysis, CD8, C-reactive protein (CRP), and CD68 (Abcam, Cambridge, UK, 1:200 dilution) antibodies were used to identify cytotoxic T-cells, monocytes, and macrophages following a routine protocol. The number of positive cells was counted each week. The remaining half of each tissue was prepared for real-time PCR analysis. Primer sequences

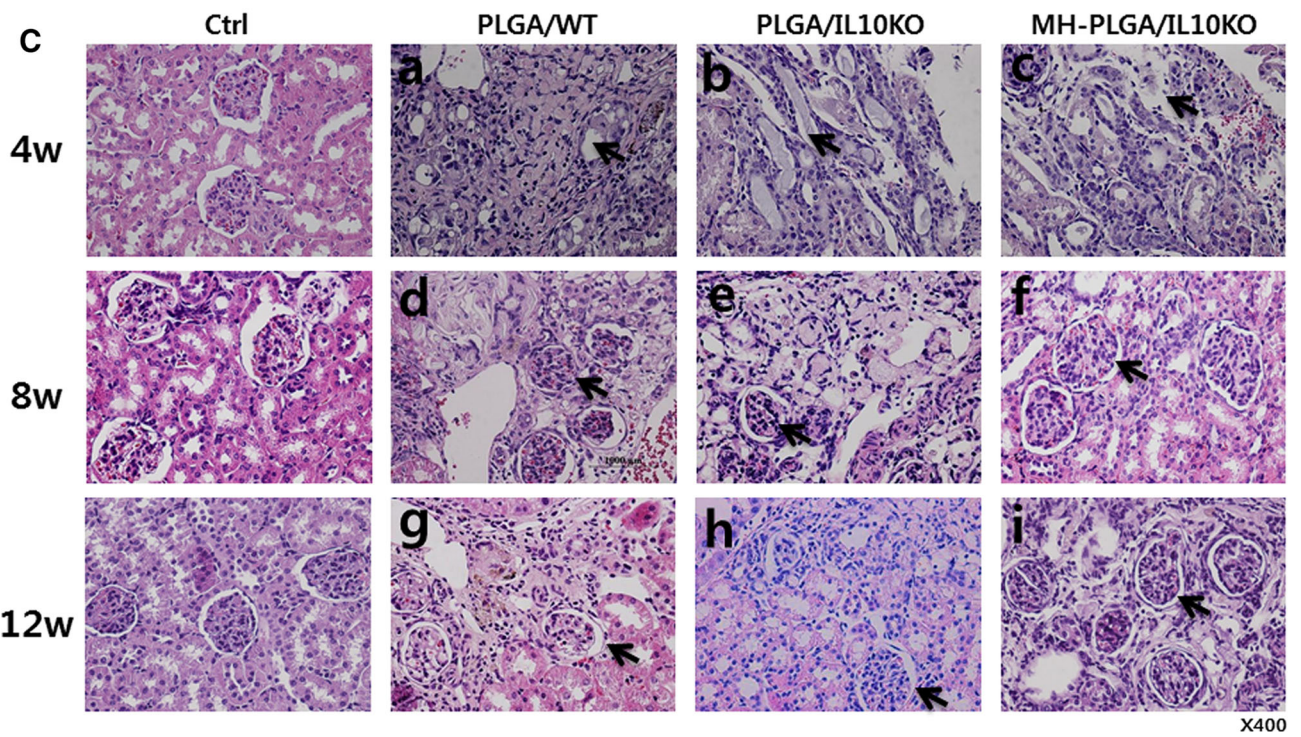
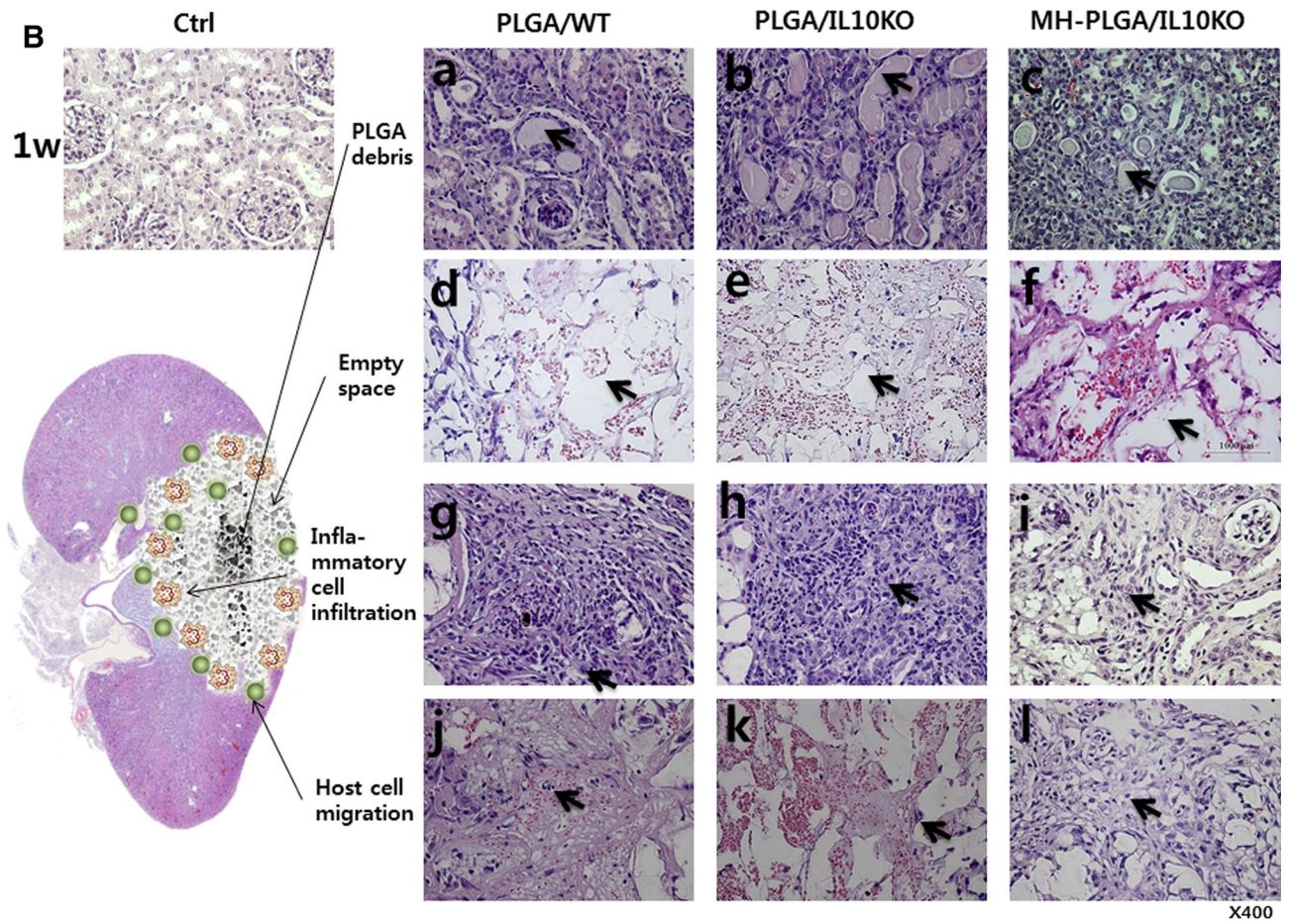
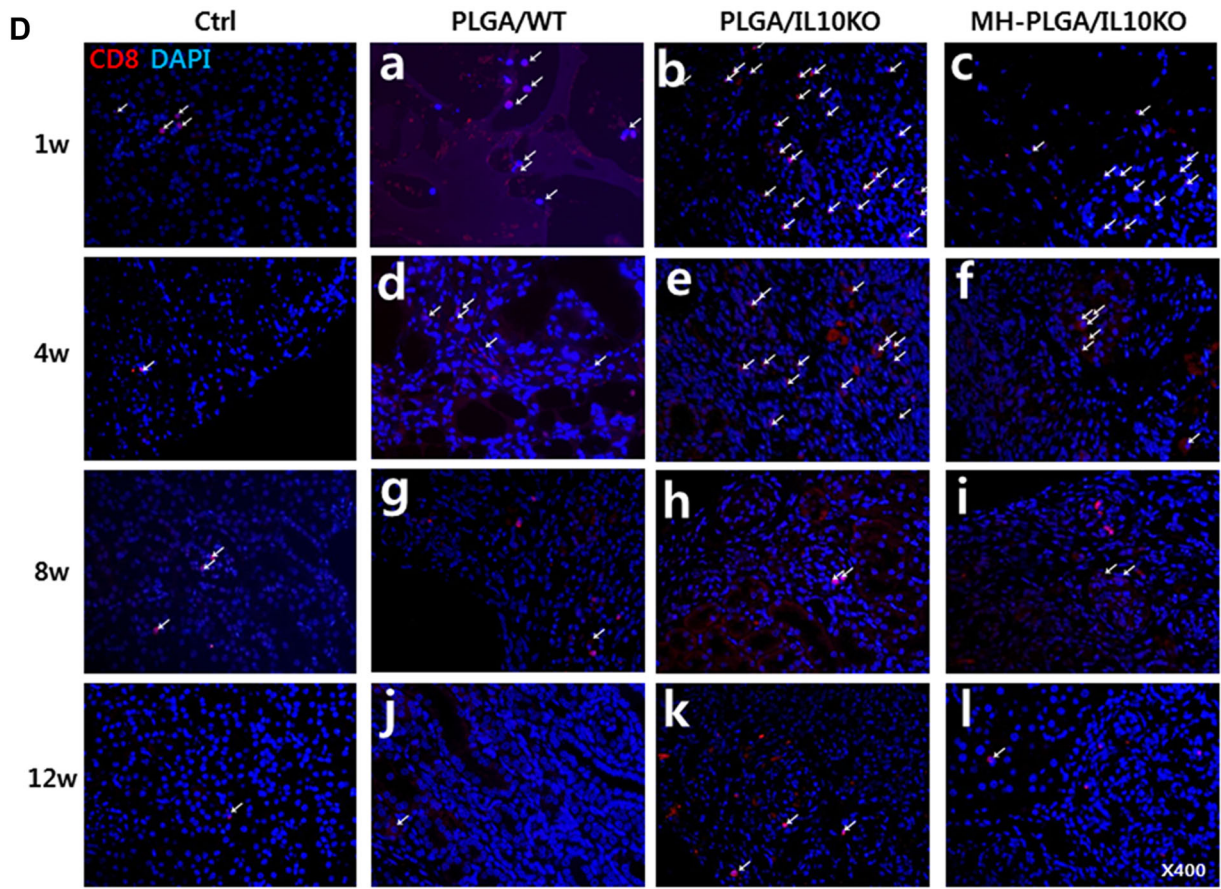


Fig. 2 continued



CD8

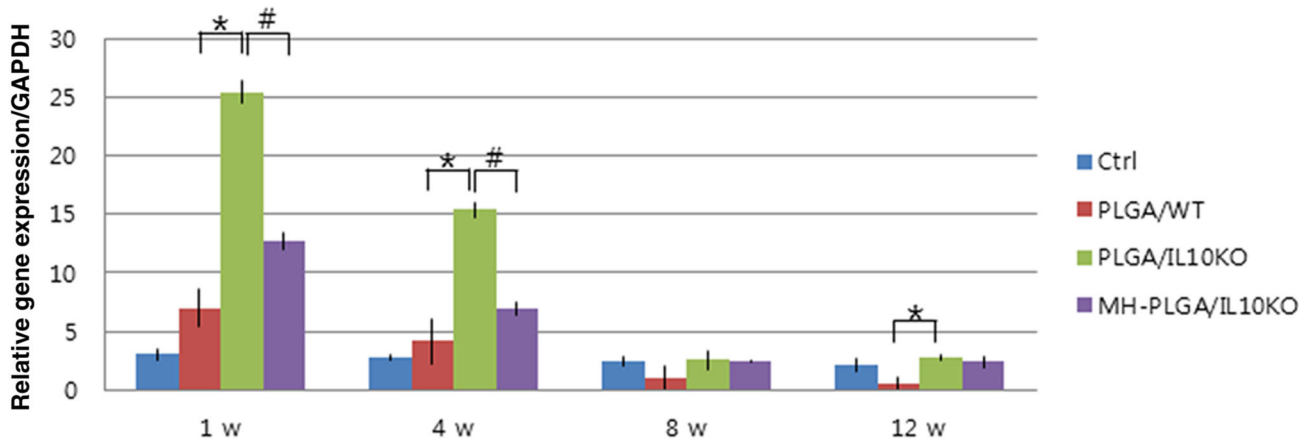
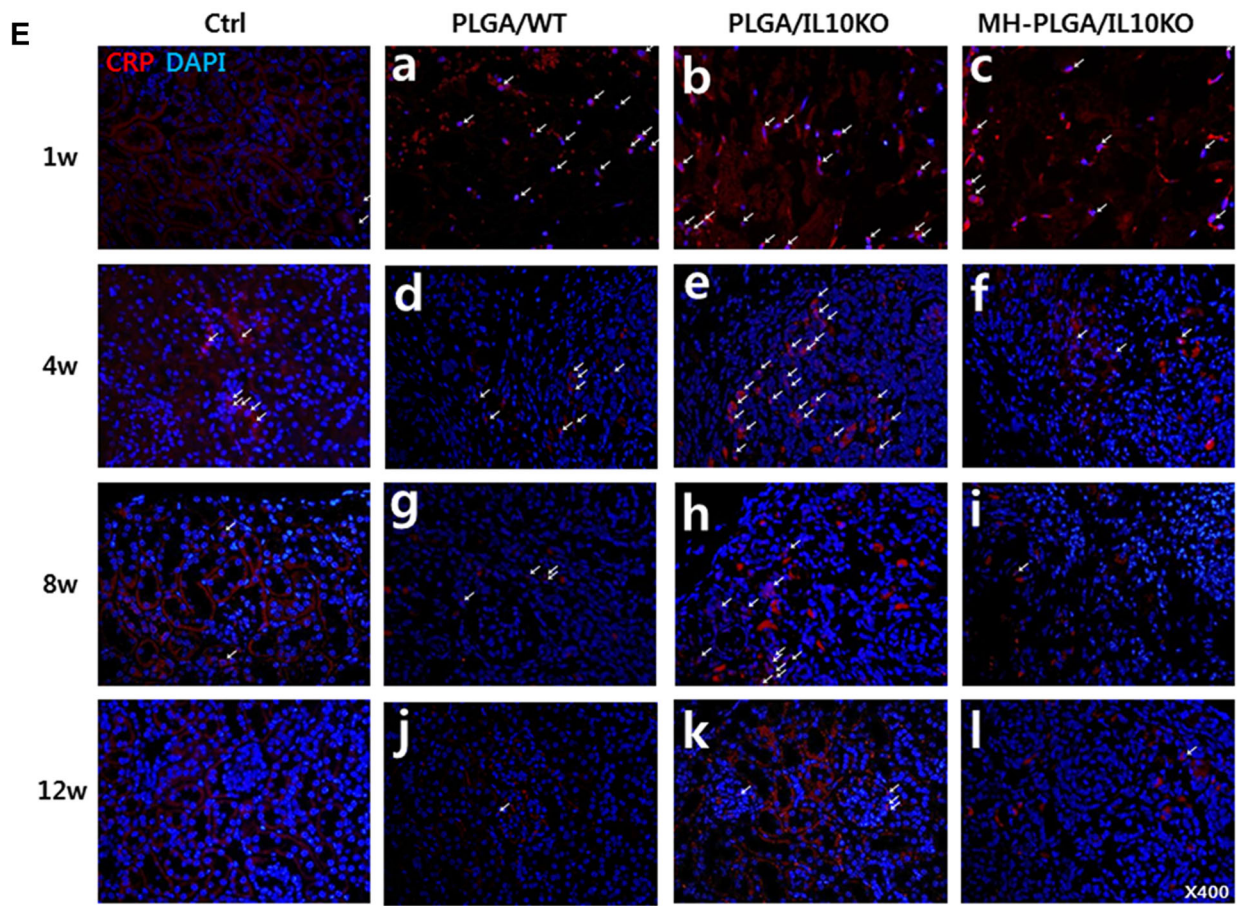


Fig. 2 continued



CRP

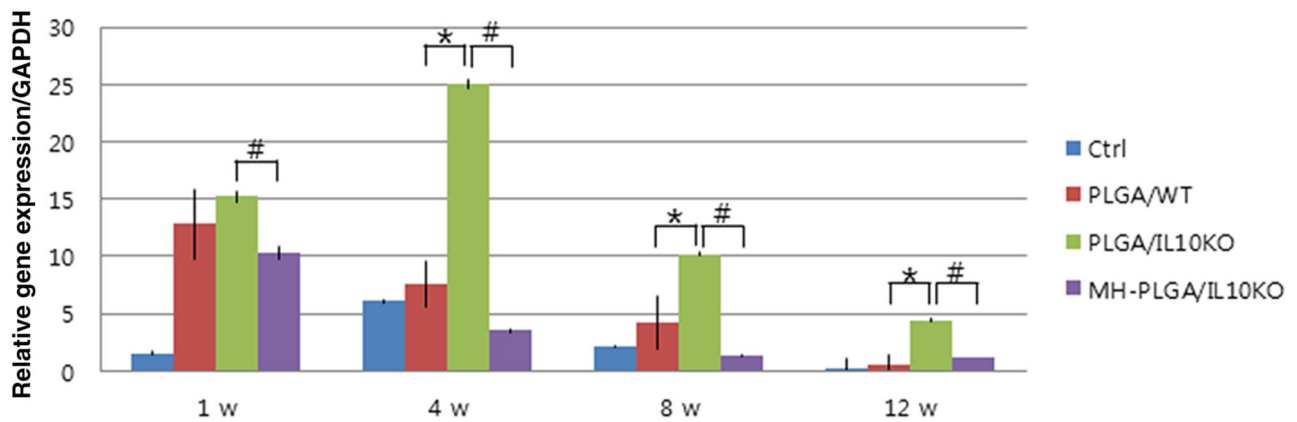


Fig. 2 continued

of the candidate and housekeeping genes are shown in Table 1. The conditions for PCR using SYBR Green (Applied Biosystems, Waltham, MA, USA) were: 95 °C for 10 min, followed by 45 cycles of 95 °C for 10 s, 58 °C

for 50 s, and 72 °C for 20 s. To analyze the relative changes in gene expression, the $2^{-\Delta\Delta C_t}$ method was used, and mRNA levels were normalized to GAPDH levels.

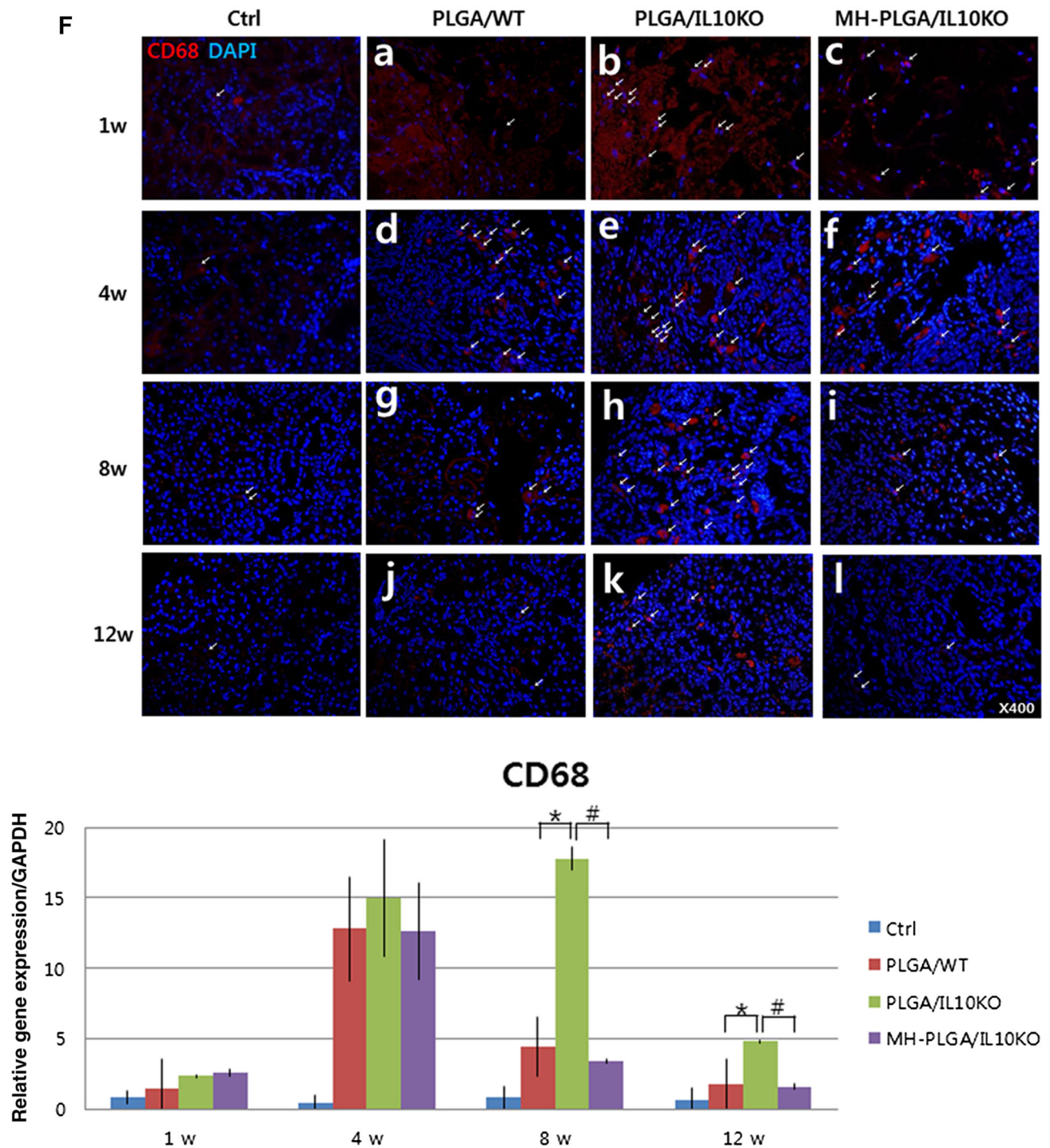


Fig. 2 continued

2.4 Statistical analysis

Quantitative data calculations were performed in Microsoft Excel (Microsoft, Redmond, WA, USA). Averaged data are presented as the mean \pm standard deviation (SD).

Two-tailed unpaired Student's *t*-tests were used to compare the means of the control and experimental groups. One-way analysis of variance multiple-comparison tests with Tukey's tests were performed; *P* values < 0.05 were considered significant.

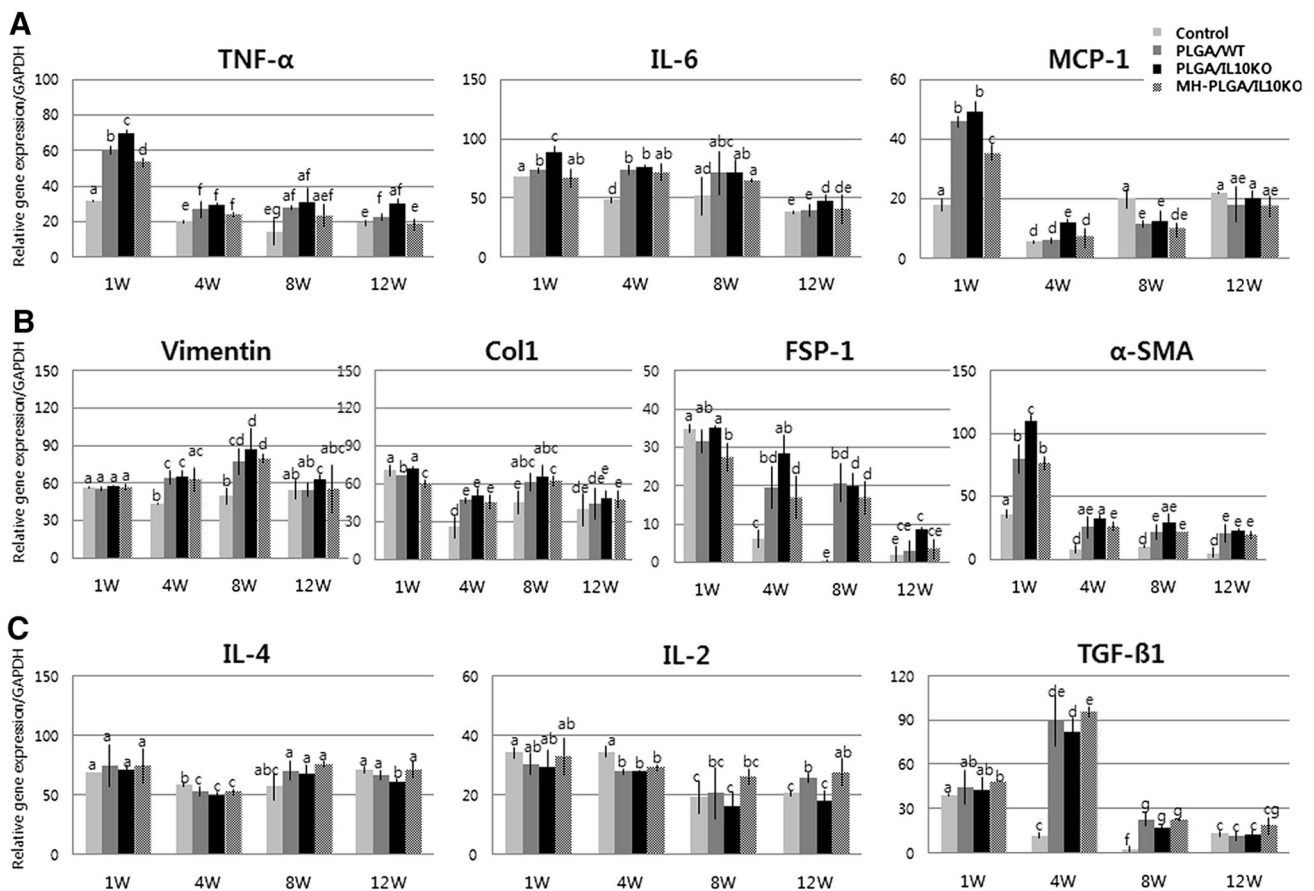


Fig. 3 Real-time PCR analysis of inflammation, fibrosis, and renal regeneration-related gene expression. **A** Pro-inflammatory cytokine gene expression. **B** Fibrosis-related gene expression. **C** Anti-inflammatory cytokine gene expression. **D** Renal regeneration-related gene expression. The alphabet on the bar indicates statistical significance,

when the differences of each group are 0.05 or less, it is written with different alphabet. Control, sham-operated C57BL/6 mice; PLGA/WT, PLGA scaffold-implanted C57BL/6 mice; PLGA/IL10KO, PLGA scaffold-implanted IL-10KO mice; MH-PLGA/IL10KO, Mg(OH)₂-incorporated PLGA scaffold implanted IL-10KO mice

3 Results

3.1 Inflammation sensitivity of IL-10 KO mice

In gross images, IL-10 KO kidneys appeared to shrink compared to WT kidneys over time (Fig. 2A). At week 1, the amount of residual PLGA was significantly higher in IL-10 KO mice than in WT mice. At week 4, the scaffolds were nearly degraded and rarely observed by direct observation. From week 8 onward, the scaffold disappeared, and different sized scars remained at the scaffold implantation region.

In histological analysis, as shown in Fig. 2B (H&E staining), IL-10 KO kidneys showed more PLGA acidic debris inside the scaffold-implanted region and less empty space (by PLGA degradation) at the scaffold margin at week 1 compared to the WT kidneys. This acidic debris enhanced inflammatory cell infiltration in the IL-10 KO kidney compared to the WT. In the acidic environment, IL-10 KO kidneys showed inhibited kidney progenitor cell

migration (k) from surrounding host tissues compared to WT. At week 4 (Fig. 2C), PLGA debris and immune cells remained in the IL-10 KO group, while, WT showed nearly no debris and migrated renal cells filled the empty space. At week 8, the IL-10 KO group formed glomeruli, but their number and size were lower than that in the WT group. This pattern was continued at week 12. No experimental groups showed calcification or abnormal tissue formation at the scaffold-implanted region.

IHC analysis was performed to identify the types of infiltrated inflammatory cells and cell morphology was determined by a pathologist. Cytotoxic T-cells were detected with a CD8 antibody (Fig. 2D). CD8⁺ cells have a small lymphocyte-like or phagocyte-like appearance, and were mainly located in the areas adjacent to the scaffold. The IL-10 KO group showed an approximately four fold higher frequency of positive cells than the WT group at week 1, and positive cell numbers decreased gradually over time in both groups. Monocytes were identified with a CRP antibody (Fig. 2E), and these cells were predominant in IL-

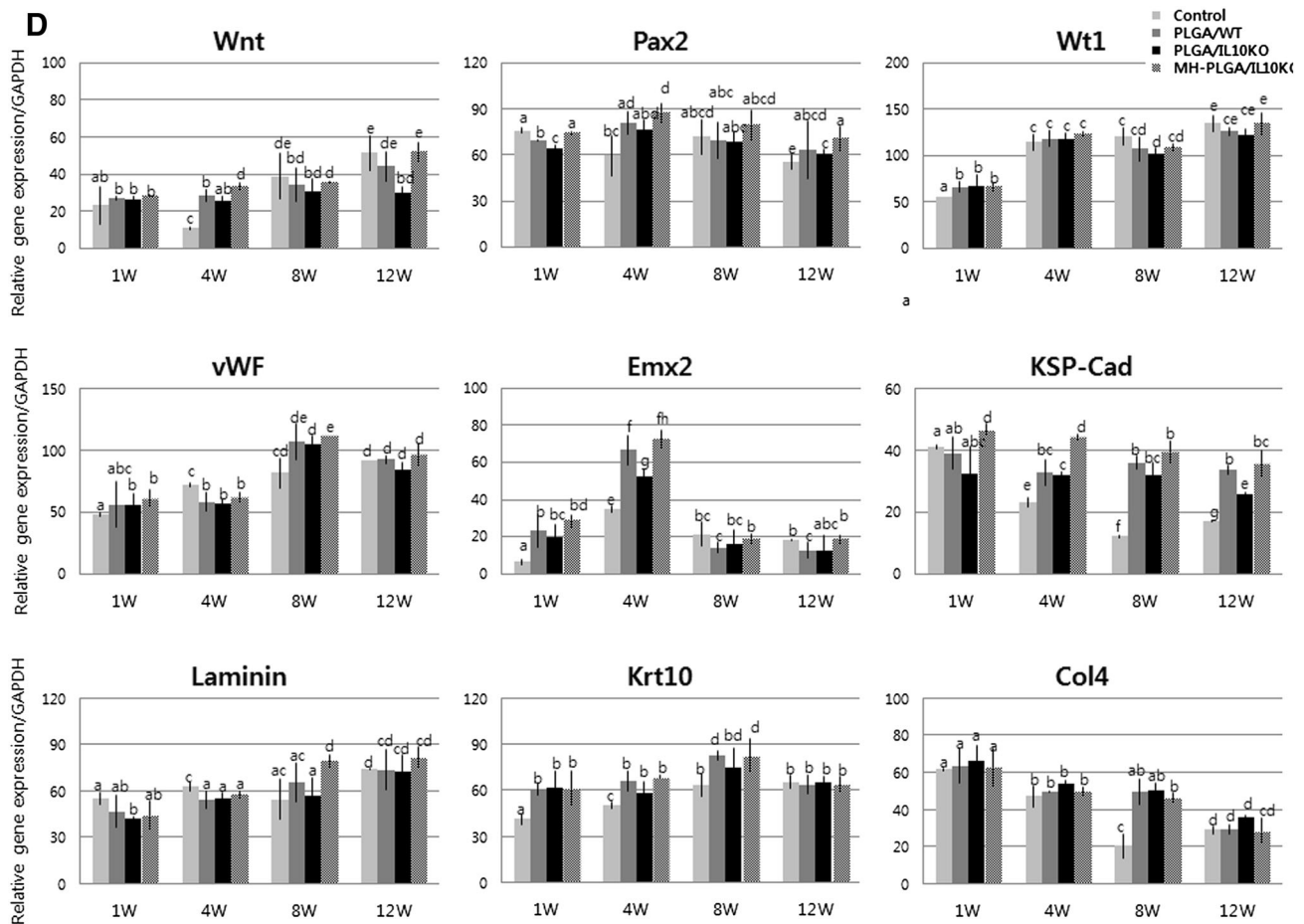


Fig. 3 continued

10 KO at weeks 1 and 4, while the WT group showed reduced positive cells for 12 weeks. Phagocytic macrophages (differentiated from monocytes) were detected using a CD68 antibody (Fig. 2F), and their expression was frequently observed in IL-10 KO mice at weeks 1, 4, and 8 compared to WT mice, indicating persistent chronic inflammation in IL-10 KO mice. The number of positive cells on IHC was quantified.

Increased inflammatory genes and fibrotic factor expression in IL-10 KO mice were detected by real-time PCR (Fig. 3A). As inflammatory response genes, tumor necrosis factor (TNF)- α , IL-6, and monocyte chemoattractant protein (MCP)-1 expression levels were higher in the PLGA/IL-10 KO group than in the WT group throughout the experimental period. Fibrosis-related factors (Fig. 3B) also showed high expression of vimentin, collagen type I, fibroblast-specific protein-1, and α -smooth muscle actin in the PLGA/IL-10 KO group compared to in the WT group. However, the expression of anti-inflammatory genes, such as IL-4, IL-2, and transforming growth factor- β 1, was low in the PLGA/IL-10 KO group compared to in the WT group (Fig. 3C). These real-time PCR results

confirmed that IL-10 KO mice are more sensitive to inflammation and fibrosis than are C57BL/6 mice.

Reduced initial inflammatory responses can promote host stem cell recruitment and tissue regeneration, and thus stem cell and renal development-related gene expression indicates inflammation sensitivity. In this analysis (Fig. 3D), PLGA/IL-10 KO mice showed relatively low expression of mesenchymal (Wnt), renal progenitor (Pax2), nephrogenesis (Wt1), glomerular endothelial (vWF), early epithelial (Emx2), tubular epithelial (KSP-Cad), cortical (laminin), and renal epithelial (Krt10) markers compared to the WT group, and the expression of Col4 (pathogenic marker) was high in the PLGA/IL-10 KO group.

3.2 Anti-inflammatory effect of MH-PLGA scaffold

Gross images (Fig. 2A) revealed that the MH-PLGA scaffold (implanted in IL-10 KO mice) showed more swelling at week 1, and then degraded faster throughout the entire observation period compared with the PLGA scaffold. In histological analysis (Fig. 2B, C), the MH-PLGA scaffold showed reduced PLGA debris, wide empty space,

low inflammatory cell infiltration, and enhanced renal progenitor cell migration compared to the PLGA scaffold at week 1. At week 4 (Fig. 2C), the MH-PLGA scaffold showed reduced PLGA debris and immune cell residue, and the formation of glomeruli and renal tubule precursors began early compared to with the PLGA scaffold. From week 8, the number/size of glomeruli and blood vessels formed were higher in the MH-PLGA scaffold than in the PLGA scaffold. Calcification or abnormal tissues were not formed for the MH-PLGA scaffold.

In IHC analysis with CD8, CRP, and CD68 antibodies to identify immune cell infiltration as inflammatory reactions (Fig. 2D–F), the MH-PLGA scaffold showed significantly reduced positive cell expression at weeks 1 and 4 compared to the PLGA scaffold. These results indicate that Mg(OH)₂ incorporation into PLGA effectively inhibited the inflammatory response. In analysis of inflammatory and fibrotic gene expression by real-time PCR (Fig. 3A, B), the MH-PLGA scaffold showed reduced expression of these genes compared to the PLGA scaffold, while anti-inflammatory gene expression was higher than in PLGA (Fig. 3C). This decreased inflammatory and fibrotic response resulted in increased expression of renal differentiation-related genes in the MH-PLGA scaffold (Fig. 3D).

These results suggest that IL-10 KO mice are an appropriate model for assessing the sensitivity of inflammation and fibrosis and that the Mg(OH)₂-incorporated PLGA scaffold has anti-inflammatory effects.

4 Discussion

To obtain a suitable *in vivo* animal model for anti-inflammatory scaffold studies, we evaluated IL-10 KO mice. In gross image analysis, PLGA implanted IL-10 KO mice showed increased kidney shrinking compared to WT mice from week 4, and the shrinkage gradually increased over time and was mostly caused by fibrosis [14]. Renal fibrosis had a direct adverse effect on the restoration of renal function after injury. According to Jin et al. [15], IL-10 enhances renal fibrosis through severe tubular injury, collagen deposition, and higher expression of pro-fibrotic genes. In our PCR results, IL-10 KO mice showed enhanced pro-fibrotic genes (vimentin, collagen I, fibroblast-specific protein-1, and α -smooth muscle actin) expression compared to WT mice. Additionally, IL-10 KO mice showed relatively severe scarring caused by fibrosis, which can cause progressive renal dysfunction leading to end-stage renal failure [14].

In histological analysis, IL-10 KO mice kidneys showed more PLGA acidic debris than WT kidneys. The factors affecting PLGA degradation are polymer composition, crystallinity, molecular weight, matrix size and shape, pH

and enzymes [16]. In our experiment, enzymes are an important factor affecting *in vivo* PLGA degradation, as the other factors were fixed. IL-10 deficiency promotes the expression of pro-inflammatory factors, which diminishes the level of enzymes such as amylase, lipase, and others [17]. There are no specific reports of renal enzyme validation, but IL-10 deficiency is thought to be affected by renal enzyme activity involved in PLGA degradation, and further studies are needed.

The long-term presence of residual acidic PLGA debris accelerates the inflammatory response. Although inflammation is an essential part of the healing process, excessive and chronic inflammation can create an unsuitable micro-environment for target tissue regeneration [18]. Histological, IHC, and real-time PCR analyses demonstrated that IL-10 KO mice had more severe inflammatory cell infiltration (T cells, monocytes, and macrophages) and higher expression of pro-inflammatory cytokines and chemokines (TNF- α , IL-6, and MCP-1) against PLGA debris compared to in WT mice. Such severe and chronic inflammatory responses promoted renal fibrosis and inhibited renal progenitor cell or stem cell migration, resulting in delayed glomeruli and renal tubule regeneration. Based on these results, IL-10 KO leads to more severe renal inflammatory response and fibrosis in the PLGA implant animal.

Next, the anti-inflammatory effect of the Mg(OH)₂-incorporated PLGA scaffold was compared to that of the PLGA scaffold in IL-10 KO mice. MH-PLGA scaffold-implanted kidneys showed more kidney shrinkage and scar formation, more swollen and rapid PLGA degradation, and significantly reduced PLGA debris compared to PLGA implanted kidneys because of the properties of Mg(OH)₂. The inflammatory responses caused by acidic PLGA products were neutralized and rapidly washed out by Mg(OH)₂ [19]. This neutralization and rapid removal of by-products reduced the influx of inflammatory cells [20, 21] and secretion of pro-inflammatory cytokines [22]. Reduced inflammation has been shown to promote mesenchymal stem cell-mediated target tissue regeneration [23]. This reduced inflammatory response maintained the survival of renal stem/progenitor cells migrating from surrounding host tissue and promoted the attachment of circulating stem cells to injured kidneys. Renal stem/progenitor cell migration was demonstrated by gene expression analysis. The Wnt (mesenchymal), Pax2 (renal progenitor), Wt1 (nephrogenesis), vWF (glomerular endothelial), Emx2 (early epithelial), KSP-Cad (tubular epithelial), laminin (cortical), and Krt10 (renal epithelial) genes were significantly increased in the MH-PLGA scaffold. These results suggest that the Mg(OH)₂-incorporated PLGA scaffold has anti-inflammatory properties.

In conclusion, the present study suggests that IL-10 KO mice are sensitive to inflammation and fibrosis induced by

the PLGA scaffold, and therefore IL-10 KO mice are an appropriate animal model for investigating the anti-inflammatory and tissue regenerative effects of the Mg(OH)₂-incorporated PLGA scaffold.

Acknowledgements This research was supported by the Basic Science Research Program through the National Research Foundation of Korea (NRF), which is funded by the Ministry of Science and ICT (2014M3A9D3034164, 2015R1C1A1A01053509 and 2016R1C1B1011180), the Ministry of Education (2015R1D1A3A03020378) and the Ministry of Trade, Industry and Energy (R0005886).

Compliance with ethical standards

Conflict of interest The authors declare that they have no conflict of interest.

Ethical statement This study was approved by the Ethics Committee of the Kyungpook National University School of Medicine (No. KNUMC 2016-05-021). This study was performed in accordance with the ethical standards laid down in the 1964 Declaration of Helsinki and its later amendments.

References

- Sundelacruz S, Kaplan DL. Stem cell- and scaffold-based tissue engineering approaches to osteochondral regenerative medicine. *Semin Cell Dev Biol*. 2009;20:646–55.
- Soler R, Fullhase C, Atala A. Regenerative medicine strategies for treatment of neurogenic bladder. *Therapy*. 2009;6:177–84.
- Prescott C, Polak DJ. The delivery of regenerative medicines and their impact on healthcare. Boca Raton: CRC Press; 2010.
- O'Brien FJ. Biomaterials and scaffolds for tissue engineering. *Mater Today (Kidlington)*. 2011;14:88–95.
- Wu XS, Wang N. Synthesis, characterization, biodegradation, and drug delivery application of biodegradable lactic/glycolic acid polymers. Part II: biodegradation. *J Biomater Sci Polym Ed*. 2001;12:21–34.
- Sung HJ, Meredith C, Johnson C, Galis ZS. The effect of scaffold degradation rate on three-dimensional cell growth and angiogenesis. *Biomaterials*. 2004;25:5735–42.
- Baraniak PR, McDevitt TC. Stem cell paracrine actions and tissue regeneration. *Regen Med*. 2010;5:121–43.
- Lee HW, Seo SH, Kum CH, Park BJ, Joung YK, Son TI, et al. Fabrication and characteristics of anti-inflammatory magnesium hydroxide incorporated PLGA scaffolds formed with various porogen materials. *Macromol Res*. 2014;22:210–8.
- National Research Council (US) Subcommittee on flame-retardant chemicals. Toxicological risks of selected flame-retardant chemicals. Magnesium hydroxide, chap. 7, vol. 7. National Academies Press; 2000. p. 131–48.
- Pan D, Kenway-Lynch CS, Lala W, Veazey RS, Lackner AA, Das A, et al. Lack of interleukin-10-mediated anti-inflammatory signals and upregulated interferon gamma production are linked to increased intestinal epithelial cell apoptosis in pathogenic simian immunodeficiency virus infection. *J Virol*. 2014;88:13015–28.
- MacDonald TT. Gastrointestinal inflammation: inflammatory bowel disease in knockout mice. *Curr Biol*. 1994;4:261–3.
- Rennick D, Davidson N, Berg D. Interleukin-10 gene knock-out mice: a model of chronic inflammation. *Clin Immunol Immunopathol*. 1995;76:S174–8.
- Kühn R, Löhler J, Rennick D, Rajewsky K, Müller W. Interleukin-10-deficient mice develop chronic enterocolitis. *Cell*. 1993;75:263–74.
- Hewitson TD. Fibrosis in the kidney: is a problem shared a problem halved? *Fibrogenesis Tissue Repair*. 2012;5:S14.
- Jin Y, Liu R, Xie J, Xiong H, He JC, Chen N. Interleukin-10 deficiency aggravates kidney inflammation and fibrosis in the unilateral ureteral obstruction mouse model. *Lab Invest*. 2013;93:801–11.
- Makadia HK, Siegel SJ. Poly lactic-co-glycolic acid (PLGA) as biodegradable controlled drug delivery carrier. *Polymers*. 2011;3:1377–97.
- Rongione AJ, Kusske AM, Reber HA, Ashley SW, McFadden DW. Interleukin-10 reduces circulating levels of serum cytokines in experimental pancreatitis. *J Gastrointest Surg*. 1997;1:159–66.
- Martin P, Leibovich SJ. Inflammatory cells during wound repair: the good, the bad and the ugly. *Trends Cell Biol*. 2005;15:599–607.
- van der Giessen WJ, Lincoff AM, Schwartz RS, van Beusekom HM, Serruys PW, Holmes DR Jr, et al. Marked inflammatory sequelae to implantation of biodegradable and nonbiodegradable polymers in porcine coronary arteries. *Circulation*. 1996;94:1690–7.
- Cherreddy KK, Vandermeulen G, Pr at V. PLGA based drug delivery systems: promising carriers for wound healing activity. *Wound Repair Regen*. 2016;24:223–36.
- Grinstein S, Swallow CJ, Rotstein OD. Regulation of cytoplasmic pH in phagocytic cell function and dysfunction. *Clin Biochem*. 1991;24:241–7.
- Lee GH, Hwang JD, Choi JY, Park HJ, Cho JY, Kim KW, et al. An acidic pH environment increases cell death and pro-inflammatory cytokine release in osteoblasts: the involvement of BAX inhibitor-1. *Int J Biochem Cell Biol*. 2011;43:1305–17.
- Liu Y, Wang L, Kikuri T, Akiyama K, Chen C, Xu X, et al. Mesenchymal stem cell-based tissue regeneration is governed by recipient T lymphocytes via IFN- γ and TNF- α . *Nat Med*. 2011;17:1594–601.